Educational Course: Translational Pathways & Validation

Mapping blood flow and tissue oxygenation with MRI: Insights from other modalities

Emmanuel L. Barbier, Ph.D
Grenoble Institut des Neurosciences (GIN)
U836 INSERM – UJF
Grenoble, France
emmanuel.barbier@ujf-grenoble.fr
http://neurosciences.ujf-grenoble.fr/equipe5

Imaging brain function is a key feature of MRI. Beyond structural parameters such as the blood volume fraction or the direction of a fiber bundle, MRI methods have been developed to map blood flow or tissue oxygenation. To challenge the results obtained by MRI, one cannot simply rely on standard histology: post-mortem, blood does not flow anymore and the oxygen is gone!

Several techniques are however available to obtain these physiological maps. One can either use clinical-like techniques such as positron emission tomography (PET) or animal specific techniques. In this presentation, we will describe some methods available to challenge MRI estimates and review results obtained by MRI and its challengers.

Blood flow

With MRI, blood flow can be mapped using several techniques, the most widely used approaches being dynamic susceptibility contrast (DSC) and arterial spin labeling (ASL) (1).

Quantitative autoradiography. One of the oldest techniques to obtain quantitative blood maps is quantitative autoradiography (2,3). One injects intravenously a freely diffusible tracer (e.g. iodoantipyrine or HMPOA) labeled with a radioactive compound (^{14}C, ^{99m}Tc…) or radioactive microspheres (but the analysis is then different from that of a freely diffusible tracer). During the injections, one samples the arterial blood (to collect an arterial input function), and, at the end of the injection, one collect the brain. Brain slices are then placed over a film or in a beta-imager to obtain autoradiography. Using the arterial input function and the map of accumulated tracer in the brain, one can derive a map of blood flow. Autoradiography has been used to challenge blood flow estimates obtained with ASL (4-6). In 2005, Ewing reported that ASL cerebral blood flows were above (34%) that reported by autoradiography (7).

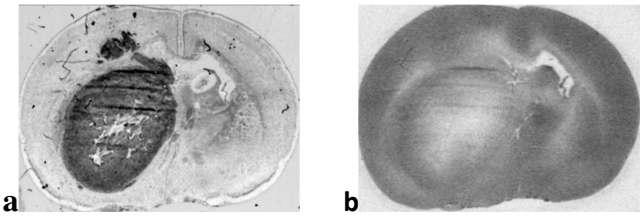

Rat bearing a C6 glioma. **a**) Hematoxylin – erythrosine staining. **b**) Corresponding ^{14}C autoradiography, a relative map of cerebral blood flow. Quantitative may be achieved using an arterial input function.

Perfusion CT. One can map perfusion using X-ray, as performed in clinic. One monitors the passage of an iodine bolus. The relation between the signal and the iodine concentration is linear. Besides this

advantage, issues raised in dynamic susceptibility imaging (e.g. choice of arterial input function, deconvolution method) are the same between perfusion CT and MRI. Perfusion CT was performed in rodent using clinical CT (8) or synchrotron radiation (9).

Positron emission tomography can also provide maps of blood flow, either using radioactive microspheres (10) or ^{15}O-labeled gases (^{15}O-CO_2 and $^{15}O_2$) (11,12). To ease the arterial input function sampling, Ose et al. used an arterio-venous shunt (11). In human, PET studies have also been performed to challenge blood flow maps obtained with MRI (13).

Optical techniques such as Near Infrared Spetroscopy (NIRS) or diffuse optical tomography (DOT) also allows an access to some blood flow information (14). One illuminates the tissue with an array of light sources and collects and analyzes the light emerging from the tissue. To obtain quantitative values, one uses an optical contrast agent such as indocyanine green (15-17). Beyond in vivo acquisition, optical means of course allow much higher spatial resolution (18). This approach is non-ionizing. Its spatial resolution is however much lower than that of perfusion CT or MRI.

Brain oxygenation

Using MRI, one can assess absolute tissue partial pressure of oxygen (e.g. FREDOM (19)) or change in tissue pO2 (e.g. MODILE, (20), blood oxygen saturation (21,22), or do MRI of Oxygen (^{17}O) (23).

Ex vivo, there are several indirect markers of hypoxia such as Pimonidazole, CA IX, Glut 1 (24). In vivo, one finds an equivalent to pimonidazole: the ^{18}F-Miso, imaged by PET (25). In vivo, one can rely on blood gases, sampled in vessels in the vicinity of the organ of interest. It is however invasive to collect arterial and venous blood gases.

PET (*cf*. above) can be used to map oxygen Extraction Fraction (OEF) and Cerebral Metabolic Rate of Oxygen ($CMRO_2$) (12,26).

Electron Paramagnetic Resonance Imaging (EPRI) can provide pO_2 maps with a high spatial resolution (27-30). It requires nitroxides or trityl radicals (e.g. triarylmethyl, TAM). From the oxygen-induced spectral broadening of TAM, pO_2 maps can be derived.

Optical techniques such as Near Infrared Spetroscopy (NIRS) or diffuse optical tomography (DOT) also allows an access to tissue oxygen saturation (14). Optical techniques however can go towards much higher spatial resolution (31,32).

References

1. Wintermark M, Sesay M, Barbier E, Borbely K, Dillon WP, Eastwood JD, Glenn TC, Grandin CB, Pedraza S, Soustiel JF, Nariai T, Zaharchuk G, Caille JM, Dousset V, Yonas H. Comparative overview of brain perfusion imaging techniques. Stroke 2005;36(9):e83-e99.
2. Branson H, Hansborough LA. The Quantitative Theory of Autoradiography Illustrated Through Experiments With P32 in the Chick Embryo. Science 1948;108(2804):327-328.
3. Sakurada O, Kennedy C, Jehle J, Brown JD, Carbin GL, Sokoloff L. Measurement of local cerebral blood flow with iodo [14C] antipyrine. The American journal of physiology 1978;234(1):H59-66.

4. Tsekos NV, Zhang F, Merkle H, Nagayama M, Iadecola C, Kim SG. Quantitative measurements of cerebral blood flow in rats using the FAIR technique: correlation with previous iodoantipyrine autoradiographic studies. Magn Reson Med 1998;39(4):564-573.
5. Ewing JR, Wei L, Knight RA, Pawa S, Nagaraja TN, Brusca T, Divine GW, Fenstermacher JD. Direct comparison of local cerebral blood flow rates measured by MRI arterial spin-tagging and quantitative autoradiography in a rat model of experimental cerebral ischemia. J Cereb Blood Flow Metab 2003;23(2):198-209.
6. Wittlich F, Kohno K, Mies G, Norris DG, Hoehn-Berlage M. Quantitative measurement of regional blood flow with gadolinium diethylenetriaminepentaacetate bolus track NMR imaging in cerebral infarcts in rats: validation with the iodo[14C]antipyrine technique. Proceedings of the National Academy of Sciences of the United States of America 1995;92(6):1846-1850.
7. Ewing JR, Cao Y, Knight RA, Fenstermacher JD. Arterial spin labeling: validity testing and comparison studies. J Magn Reson Imaging 2005;22(6):737-740.
8. Kan Z, Phongkitkarun S, Kobayashi S, Tang Y, Ellis LM, Lee TY, Charnsangavej C. Functional CT for quantifying tumor perfusion in antiangiogenic therapy in a rat model. Radiology 2005;237(1):151-158.
9. Adam JF, Nemoz C, Bravin A, Fiedler S, Bayat S, Monfraix S, Berruyer G, Charvet AM, Le Bas JF, Elleaume H, Esteve F. High-resolution blood-brain barrier permeability and blood volume imaging using quantitative synchrotron radiation computed tomography: study on an F98 rat brain glioma. J Cereb Blood Flow Metab 2005;25(2):145-153.
10. Bos A, Bergmann R, Strobel K, Hofheinz F, Steinbach J, den Hoff J. Cerebral blood flow quantification in the rat: a direct comparison of arterial spin labeling MRI with radioactive microsphere PET. EJNMMI research 2012;2(1):47.
11. Ose T, Watabe H, Hayashi T, Kudomi N, Hikake M, Fukuda H, Teramoto N, Watanabe Y, Onoe H, Iida H. Quantification of regional cerebral blood flow in rats using an arteriovenous shunt and micro-PET. Nuclear medicine and biology 2012;39(5):730-741.
12. Watabe T, Shimosegawa E, Watabe H, Kanai Y, Hanaoka K, Ueguchi T, Isohashi K, Kato H, Tatsumi M, Hatazawa J. Quantitative evaluation of cerebral blood flow and oxygen metabolism in normal anesthetized rats: 15O-labeled gas inhalation PET with MRI Fusion. Journal of nuclear medicine : official publication, Society of Nuclear Medicine 2013;54(2):283-290.
13. Ye FQ, Berman KF, Ellmore T, Esposito G, van Horn JD, Yang Y, Duyn J, Smith AM, Frank JA, Weinberger DR, McLaughlin AC. H(2)(15)O PET validation of steady-state arterial spin tagging cerebral blood flow measurements in humans. Magnetic Resonance in Medicine 2000;44(3):450-456.
14. Culver JP, Durduran T, Furuya D, Cheung C, Greenberg JH, Yodh AG. Diffuse optical tomography of cerebral blood flow, oxygenation, and metabolism in rat during focal ischemia. J Cereb Blood Flow Metab 2003;23(8):911-924.
15. Kuebler WM, Sckell A, Habler O, Kleen M, Kuhnle GE, Welte M, Messmer K, Goetz AE. Noninvasive measurement of regional cerebral blood flow by near-infrared spectroscopy and indocyanine green. J Cereb Blood Flow Metab 1998;18(4):445-456.
16. Keller E, Nadler A, Alkadhi H, Kollias SS, Yonekawa Y, Niederer P. Noninvasive measurement of regional cerebral blood flow and regional cerebral blood volume by near-infrared spectroscopy and indocyanine green dye dilution. Neuroimage 2003;20(2):828-839.
17. Lin ZJ, Ren M, Li L, Liu Y, Su J, Yang SH, Liu H. Interleaved imaging of cerebral hemodynamics and blood flow index to monitor ischemic stroke and treatment in rat by volumetric diffuse optical tomography. Neuroimage 2014;85 Pt 1:566-582.
18. Lee J, Radhakrishnan H, Wu W, Daneshmand A, Climov M, Ayata C, Boas DA. Quantitative imaging of cerebral blood flow velocity and intracellular motility using dynamic light scattering-optical coherence tomography. J Cereb Blood Flow Metab 2013;33(6):819-825.

19. Mason RP, Hunjan S, Constantinescu A, Song Y, Zhao D, Hahn EW, Antich PP, Peschke P. Tumor oximetry: comparison of 19F MR EPI and electrodes. Advances in experimental medicine and biology 2003;530:19-27.
20. Jordan BF, Magat J, Colliez F, Ozel E, Fruytier AC, Marchand V, Mignion L, Bouzin C, Cani PD, Vandeputte C, Feron O, Delzenne N, Himmelreich U, Denolin V, Duprez T, Gallez B. Mapping of oxygen by imaging lipids relaxation enhancement: A potential sensitive endogenous MRI contrast to map variations in tissue oxygenation. Magn Reson Med 2012.
21. He X, Zhu M, Yablonskiy DA. Validation of oxygen extraction fraction measurement by qBOLD technique. Magn ResonMed 2008;60(4):882-888.
22. Christen T, Lemasson B, Pannetier N, Farion R, Segebarth C, Remy C, Barbier EL. Evaluation of a quantitative blood oxygenation level-dependent (qBOLD) approach to map local blood oxygen saturation. NMR Biomed 2011;24(4):393-403.
23. Pekar J, Ligeti L, Ruttner Z, Lyon RC, Sinnwell TM, van Gelderen P, Fiat D, Moonen CT, McLaughlin AC. In vivo measurement of cerebral oxygen consumption and blood flow using 17O magnetic resonance imaging. Magn Reson Med 1991;21(2):313-319.
24. Tatum JL, Kelloff GJ, Gillies RJ, Arbeit JM, Brown JM, Chao KS, Chapman JD, Eckelman WC, Fyles AW, Giaccia AJ, Hill RP, Koch CJ, Krishna MC, Krohn KA, Lewis JS, Mason RP, Melillo G, Padhani AR, Powis G, Rajendran JG, Reba R, Robinson SP, Semenza GL, Swartz HM, Vaupel P, Yang D, Croft B, Hoffman J, Liu G, Stone H, Sullivan D. Hypoxia: importance in tumor biology, noninvasive measurement by imaging, and value of its measurement in the management of cancer therapy. International journal of radiation biology 2006;82(10):699-757.
25. Corroyer-Dulmont A, Peres EA, Petit E, Durand L, Marteau L, Toutain J, Divoux D, Roussel S, MacKenzie ET, Barre L, Bernaudin M, Valable S. Noninvasive assessment of hypoxia with 3-[18F]-fluoro-1-(2-nitro-1-imidazolyl)-2-propanol ([18F]-FMISO): a PET study in two experimental models of human glioma. Biological chemistry 2013;394(4):529-539.
26. Kobayashi M, Mori T, Kiyono Y, Tiwari VN, Maruyama R, Kawai K, Okazawa H. Cerebral oxygen metabolism of rats using injectable (15)O-oxygen with a steady-state method. J Cereb Blood Flow Metab 2012;32(1):33-40.
27. Redler G, Epel B, Halpern HJ. Principal component analysis enhances SNR for dynamic electron paramagnetic resonance oxygen imaging of cycling hypoxia in vivo. Magn Reson Med 2014;71(1):440-450.
28. Shen J, Sood R, Weaver J, Timmins GS, Schnell A, Miyake M, Kao JP, Rosen GM, Liu KJ. Direct visualization of mouse brain oxygen distribution by electron paramagnetic resonance imaging: application to focal cerebral ischemia. J Cereb Blood Flow Metab 2009;29(10):1695-1703.
29. Epel B, Bowman MK, Mailer C, Halpern HJ. Absolute oxygen R imaging in vivo with pulse electron paramagnetic resonance. Magn Reson Med 2013.
30. Elas M, Williams BB, Parasca A, Mailer C, Pelizzari CA, Lewis MA, River JN, Karczmar GS, Barth ED, Halpern HJ. Quantitative tumor oxymetric images from 4D electron paramagnetic resonance imaging (EPRI): methodology and comparison with blood oxygen level-dependent (BOLD) MRI. Magn Reson Med 2003;49(4):682-691.
31. Lecoq J, Parpaleix A, Roussakis E, Ducros M, Goulam Houssen Y, Vinogradov SA, Charpak S. Simultaneous two-photon imaging of oxygen and blood flow in deep cerebral vessels. Nature medicine 2011;17(7):893-898.
32. Shonat RD, Wachman ES, Niu W, Koretsky AP, Farkas DL. Near-simultaneous hemoglobin saturation and oxygen tension maps in mouse brain using an AOTF microscope. Biophys J 1997;73(3):1223-1231.